



Skin pharmacokinetics of miltefosine in the treatment of post-kala-azar dermal leishmaniasis in South Asia

Semra Palić¹, Wan-Yu Chu ^{1,2}, Shyam Sundar³, Dinesh Mondal⁴, Pradeep Das⁵, Krishna Pandey⁵, Sheeraz Raja⁶, Suman Rijal⁶, Ignace C. Roseboom¹, Abdullah Hamadeh⁷, Paul R.V. Malik⁷, Jos H. Beijnen¹, Alwin D.R. Huitema^{1,8,9}, Erik Sjögren^{10,11}, Fabiana Alves¹² and Thomas P.C. Dorlo ^{1,2*}

¹Department of Pharmacy & Pharmacology, The Netherlands Cancer Institute—Antoni van Leeuwenhoek Hospital, Amsterdam, The Netherlands; ²Department of Pharmacy, Uppsala University, Uppsala, Sweden; ³Department of Medicine, Banaras Hindu University, Varanasi, India; ⁴Centre for Nutrition and Food Security (CNFS), International Centre for Diarrhoeal Disease Research, Bangladesh (icddr, b), Dhaka, Bangladesh; ⁵Rajendra Memorial Research Institute of Medical Sciences (RMRIMS), Patna, India; ⁶Drugs for Neglected Diseases initiative (DNDi) South Asia, New Delhi, India; ⁷School of Pharmacy, University of Waterloo, Waterloo, Ontario, Canada; ⁸Department of Pharmacology, Princess Máxima Center for Pediatric Oncology, Utrecht, The Netherlands; ⁹Department of Clinical Pharmacy, University Medical Center Utrecht, Utrecht University, Utrecht, The Netherlands; ¹⁰Department of Pharmaceutical Biosciences, Uppsala University, Uppsala, Sweden; ¹¹Pharmetheus AB, Uppsala, Sweden; ¹²Drugs for Neglected Diseases initiative (DNDi), Geneva, Switzerland

*Corresponding author. E-mail: thomas.dorlo@farmaci.uu.se

Received 21 December 2023; accepted 4 April 2024

Introduction: Post-kala-azar dermal leishmaniasis (PKDL) arises as a dermal complication following a visceral leishmaniasis (VL) infection. Current treatment options for PKDL are unsatisfactory, and there is a knowledge gap regarding the distribution of antileishmanial compounds within human skin. The present study investigated the skin distribution of miltefosine in PKDL patients, with the aim to improve the understanding of the pharmacokinetics at the skin target site in PKDL.

Methods: Fifty-two PKDL patients underwent treatment with liposomal amphotericin B (20 mg/kg) plus miltefosine (allometric dosing) for 21 days. Plasma concentrations of miltefosine were measured on study days 8, 15, 22 and 30, while a punch skin biopsy was taken on day 22. A physiologically based pharmacokinetic (PBPK) model was developed to evaluate the distribution of miltefosine into the skin.

Results: Following the allometric weight-based dosing regimen, median miltefosine concentrations on day 22 were 43.73 µg/g (IQR: 21.94–60.65 µg/g) in skin and 33.29 µg/mL (IQR: 25.9–42.58 µg/mL) in plasma. The median individual concentration ratio of skin to plasma was 1.19 (IQR: 0.79–1.9). In 87% (45/52) of patients, skin exposure was above the suggested EC₉₀ PK target of 10.6 mg/L associated with *in vitro* susceptibility. Simulations indicated that the residence time of miltefosine in the skin would be more than 2-fold longer than in plasma, estimated by a mean residence time of 604 versus 266 hours, respectively.

Conclusion: This study provides the first accurate measurements of miltefosine penetration into the skin, demonstrating substantial exposure and prolonged retention of miltefosine within the skin. These findings support the use of miltefosine in cutaneous manifestations of leishmaniasis. In combination with parasitological and clinical data, these results are critical for the future optimization of combination therapies with miltefosine in the treatment of PKDL.

Introduction

Leishmaniasis is an infectious disease caused by the protozoan parasite *Leishmania*, transmitted by sand flies. By primarily affecting the poorest populations, leishmaniasis remains one of the most neglected tropical diseases.¹ The most common clinical presentation of the disease, which affects up to 1 million people per year, is cutaneous leishmaniasis (CL), leading to skin ulcers and lesions at the site of infection.² The most severe form of leishmaniasis is visceral leishmaniasis (VL) or kala-azar.³ VL affects internal organs and is lethal within months without adequate treatment. In addition, some patients who have previously been treated for VL develop post-kala-azar dermal leishmaniasis (PKDL) months or years after treatment. Clinical manifestations of PKDL include skin rash in the form of macular, nodular or mixed lesions.^{4,5} In South Asia, PKDL develops in 5%–10% of VL patients within an average of 2 years after VL treatment, with the macular form predominating.⁴ As *Leishmania* parasites reside in the skin, sand flies feeding on PKDL patients may become infected and further transmit the parasite.^{6,7} Therefore, patients with chronic PKDL could serve as reservoirs for VL transmission, emphasizing the public health role of treating these patients.

Miltefosine is the first, and still the only, oral agent available for the treatment of leishmaniasis. It is an alkylphosphocholine compound, consisting of a long alkyl chain and a polar phosphocholine head group.⁸ Owing to its chemical structure, with a long hydrophobic tail, miltefosine has a high affinity for lipid rafts and can incorporate into the lipid bilayers of cell membranes without disrupting the membrane itself.^{9,10} With respect to pharmacokinetics (PK), miltefosine is slowly absorbed from the gastrointestinal tract, with reported saturable absorption in both preclinical and clinical studies.^{11,12} In addition, plasma clearance is low, with elimination half-lives estimated at 7–30 days.⁸ Owing to these PK properties, miltefosine accumulates in plasma until the end of treatment.^{13,14}

Treatment regimens with miltefosine have been established for CL and VL. In South Asia, the current recommended treatment for PKDL is miltefosine for a long period of 12 weeks.¹⁵ However, this long 12-week regimen, combined with potential tolerability issues, may hinder treatment compliance. In addition, women of childbearing age require 8 months of contraception (during treatment and for 5 months after treatment) due to teratogenicity.¹⁶ Recent studies have highlighted the efficacy of liposomal amphotericin B (LAmB, AmBisome[®]) alone and in combination with miltefosine for treating PKDL.^{17–21} Therefore, the latest clinical research in South Asia has been focused on investigating shortened treatment regimens involving LAmB and miltefosine for PKDL.²² Owing to a lack of studies investigating exposure-response relationships for miltefosine in the treatment of PKDL, it is difficult to further optimize and rationalize treatment. The main burden of parasite biomass in PKDL is located in the dermis of the skin, however, no investigations have been performed on target site exposure in the skin of any of the currently used antileishmanial drugs in the treatment of any type of dermal leishmaniasis.²³ Such PK studies are pivotal to further optimize and rationalize treatment regimens for the various different clinical presentations of leishmaniasis.

In this study, we aimed to provide the first data on miltefosine exposure in skin tissue from PKDL patients treated with miltefosine, as a proxy for target site exposure at the site of parasite infection. Furthermore, we used a physiologically based pharmacokinetic (PBPK) modelling approach to further elucidate miltefosine PK in both skin and plasma after oral administration, as a framework for target site tissue predictions.

Methods

Clinical studies and patient cohorts

Study in post-kala-azar dermal leishmaniasis

The clinical data originated from a non-comparative, open label, randomized phase II trial, which was conducted to assess the safety and efficacy of LAmB monotherapy (total dose of 20 mg/kg) and LAmB (20 mg/kg) in combination with miltefosine (allometric dosing) in the treatment of PKDL patients from Bangladesh (at the International Centre for Diarrhoeal Disease Research) and India (at the Rajendra Memorial Research Institute of Medical Sciences, Patna and the Kala-Azar Medical Research Centre, Muzzafarpur, both in Bihar state).²⁴ In the combination arm, the daily oral miltefosine dose was divided in two administrations (with food) according to a previously determined allometric dose for a duration of 21 days. Miltefosine allometric dosing was calculated according to patient's weight, height and sex, and was applied to patients weighing <30 kg.¹³ For patients weighing ≥30 kg, the allometric dose corresponded to the conventional dose of 2.5 mg/kg/day, with a maximum 150 mg/day. Therefore, patients weighing ≥30 to 44 kg received 100 mg/day and patients ≥45 kg received 150 mg/day.¹³

Enrolment criteria included patients with confirmed PKDL by clinical presentation and demonstration of parasites by microscopy skin smear or quantitative PCR, with documented stable or progressive disease lasting longer than 4 months. The age inclusion criteria ranged from 6 to 60 years, and written informed consent from patients, or the patient's parent or guardian for children younger than 18 years, was obtained before treatment initiation. Patients who had received treatment for PKDL in the last 2 years were not included in this study. The study further excluded pregnant and lactating women, women of childbearing potential who did not agree to take effective contraception for the duration of treatment and 5 months thereafter, patients with contaminant infection such as tuberculosis or HIV, patients with a severe underlying disease such as cardiac, renal or hepatic diseases, as well as individuals with severe malnutrition.

Miltefosine K₂EDTA plasma samples were collected on study days 8, 15, 22 and 30, as well as at 3 months during the follow-up period. In addition, on study day 22 (approximately 24 hours after the last miltefosine dose when the maximal concentration was expected) a full thickness punch biopsy of the skin was taken from all patients randomized to the LAmB/miltefosine treatment group. All samples were stored and transported frozen at a minimum of –70°C, after transport to the bioanalytical laboratory, samples were kept frozen, likewise, at a minimum of –70°C, until analysis.

Study in cutaneous leishmaniasis

Previous PK data from a study in CL patients were used to enable the development of the miltefosine PBPK model, as the PK data from the PKDL trial lacked plasma samples to accurately estimate drug absorption. Thirty-one Dutch military personnel who were infected with CL (*Leishmania major*) and were otherwise systemically healthy were included in the present analysis. A population PK analysis of this trial has been previously reported.²⁵ Plasma samples were obtained at 2, 4 and 6 hours after the first dose on the first day of treatment, then weekly

during the treatment on an outpatient basis, as well as for 5 months of follow up.²⁵

Quantification of miltefosine concentrations

In plasma

Miltefosine was quantified in K₂EDTA plasma by LC-MS/MS in both studies, previously validated with the lowest limit of quantification of 4 and 10 ng/mL for the CL and PKDL studies, respectively.²⁶ Samples from the PKDL study were measured at the bioanalytical laboratory of Lambda Therapeutic Research, in Ahmedabad, India. Samples from the CL study were measured at the bioanalytical laboratory of the Antoni van Leeuwenhoek Hospital/Netherlands Cancer Institute in Amsterdam. Both laboratories used the same methodology in terms of sample preparation techniques, following a technology transfer. Separate validations were performed locally following FDA/EMA guidelines to ensure comparability of the data.

In skin

Collected biopsies were stored at -70°C and transported on dry ice to the bioanalytical laboratory of the Antoni van Leeuwenhoek Hospital/Netherlands Cancer Institute in Amsterdam. Miltefosine was quantified in skin by LC-MS/MS. Detailed bioanalytical assay development and validation were reported in a previous publication.²⁷ The validated concentration range for a standardized 15 mg skin biopsy sample was 4–1000 ng/mL, converted into $\mu\text{g/g}$ miltefosine in skin biopsy using the mass of each individual human skin tissue sample.

PBPK model development

This work used middle-out strategies to facilitate PBPK model development. First, the PBPK model was developed based on databases containing drug-specific, system-specific parameters, and *in vitro* and preclinical data for miltefosine PK. Next, clinical data were used to optimize the model parameters.

Software

PBPK modelling was performed using the Open System Pharmacology Suite including the modelling software PK-Sim[®] and MoBi[®] (Open Systems Pharmacology Suite v.9.1, <https://www.open-systems-pharmacology.org>). Graphical evaluation and statistical analyses were performed in R and R Studio (v.3.6.3 and 3.4.3).²⁸

Miltefosine PBPK model building

Firstly, the miltefosine drug model was built using drug physicochemical properties. The model was informed by the data available on the processes of absorption, distribution, metabolism and elimination. The literature was reviewed through the PubMed database to collect drug-specific parameter values. In the case of multiple values being identified for a parameter, either a range of values was tested on the model or, when that was not possible, each value was tested for its ability to result in a simulation that adequately fitted the observed data. Parameters were identified by minimization of the residuals between observed data and corresponding simulation output, adopting the optimization functionality and the Levenberg–Marquardt algorithm included in PK-Sim[®].

Second, a full body PBPK model was built for miltefosine, adopting the generic model for small molecules within the PK-Sim[®] software. This is a full body PBPK model accommodating 15 different organs with rich information regarding the volumes, blood flow rates, metabolism etc.²⁹ Each of these organs further consists of compartments representing the plasma, interstitial and intracellular space. To further improve model performance, drug-related parameters were further optimized to align with PK data from two clinical studies of miltefosine PK in CL and PKDL

patients. Parameters were identified by minimization of the residuals between observed data and corresponding simulation output, adopting the optimization functionality and the Levenberg–Marquardt algorithm included in PK-Sim[®]. Using the pooled miltefosine plasma concentration data, distribution and elimination were parametrized by optimizing parameters such as lipophilicity, specific intestinal permeability (transcellular) and specific drug clearance (normalized to the enzyme concentration of $1\ \mu\text{mol/L}$). In addition, since miltefosine has a long hydrophobic chain, it is expected to be incorporated into the cell membrane, and subsequently enter the cell. This non-specific binding was accommodated in the model by including a non-specific binding partner located at the cell membrane. MoBi[®] was then used to facilitate simulation output representative of the clinical reference skin concentration measurements by creating an observer to trace the concentration of the drug sequestered in the cell membrane, while conserving drug mass balance within the original PBPK model. The binding of miltefosine within the cell membrane was mimicked by inclusion of a non-specific binding partner, defined by an equilibrium constant K_d and a dissociation constant k_{off} . The value of K_d was fixed at $1\ \mu\text{mol/L}$, while k_{off} and the reference concentration of this non-specific binding partner were determined based on the miltefosine concentrations measured in plasma and the skin biopsies, and was subsequently applied to other organs. Given the consistency of the membrane binding process across all organs, the same K_d and k_{off} were used assuming the same affinity throughout. Relative expressions of this binding partner in each organ were scaled by the volumes of these organs and blood flow rates.

Simulations

Several simulations were performed based on virtual patient populations representative of the patient cohorts of the clinical data included. For each of the simulations, the miltefosine dosing regimen of the corresponding clinical study was used. For this purpose, virtual populations of individuals were created, using the built-in population algorithm in PK-Sim[®] and based on the population characteristics for the respective studies. System-dependent parameters, such as age, weight, height, organ weights, blood flow rates, tissue composition etc., were varied using the algorithm implemented in PK-Sim[®].³⁰ Simulations of miltefosine in plasma and skin were used for the final parameter identification step. Finally, the optimized PBPK model was used to simulate PK profiles of miltefosine in the spleen and liver.

Results

Patients and data

In total, PK data of 52 patients were available from the PKDL study. The details of patient demographics, as well as the dosing of miltefosine, are provided in Table 1. A total of 273 miltefosine plasma concentrations and 52 skin biopsies were available for this analysis.

Observed skin penetration of miltefosine and comparison with exposure in plasma

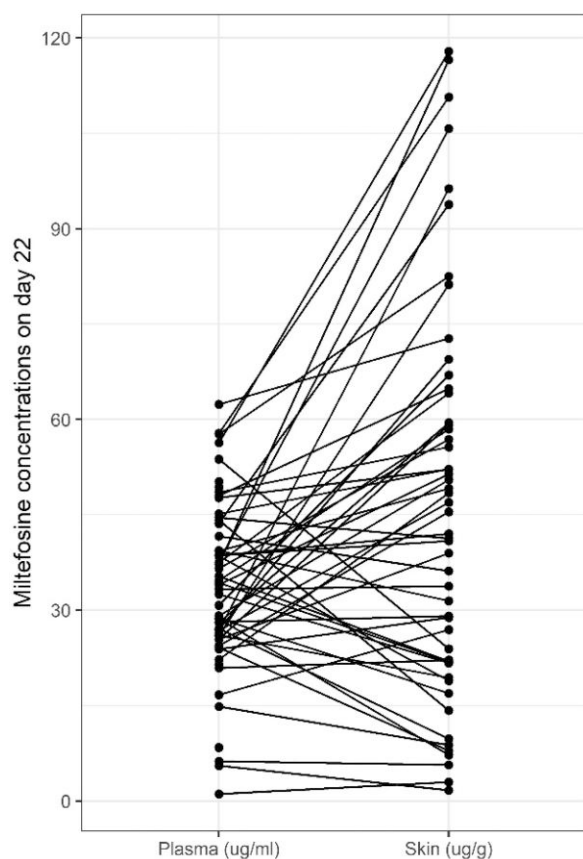
The miltefosine concentrations that were measured in the skin biopsies collected represent a combination of intracellular and interstitial concentrations, as extracellular miltefosine and dermal blood were washed off during the sample preparation. Observed miltefosine concentrations in the skin and plasma are presented in Figure 1.

Median miltefosine concentration in the skin on day 22 was $43.73\ \mu\text{g/g}$ (IQR: 21.94–60.65 $\mu\text{g/g}$) while the median concentration in plasma at the same time point was $33.29\ \mu\text{g/mL}$ (IQR: 25.9–42.58 $\mu\text{g/mL}$). High interindividual variability (IIV) in

Table 1. Patient demographics and the dosing of miltefosine in patients with PKDL included in the PBPK model development

Parameter	Median value [IQR]	
Study site	Bangladesh	India
Total number of patients	14	38
Age (years)	31.5 [13.8, 38.0]	19.5 [15.0, 31.0]
Weight (kg)	43.5 [38.3, 54.0]	45.0 [40.0, 50.8]
Height (cm)	161 [152, 164]	152 [146, 160]
Male (n, %)	9 (64.3%)	15 (39.5%)
Dose (mg/kg/day)	2.27 [1.89–2.60]	2.16 [1.87–2.39]
Baseline PKDL lesion score (no. of squares on the manikin) ^a		
Nodular or papular lesions	0 [0, 4.75]	1.50 [0, 9.50]
Macular lesions	25.5 [6.00, 135]	182 [82.8, 284]

^aPKDL lesions were quantified clinically using a trial specific diagram.³¹ The distribution of the lesions were plotted in squares on a manikin, corresponding to the affected areas.

**Figure 1.** Observed miltefosine concentrations in plasma and skin after 21-day treatment with an allometric weight-based dosing regimen. Individual patient measurements for both plasma and skin are paired by individual lines.**Table 2.** Summary of miltefosine drug model parameters used in PBPK simulations

Parameter	Value	Unit
Physiochemical parameter		
Molecular weight	407.58	g/mol
Fraction unbound in plasma (Fu)	0.03	
pK _a (acid)	2	
pK _a (base)	7.2	
Aqueous diffusion coefficient	2.9 × 10 ⁻⁴	cm ² /min
Solubility (at reference pH)	2.5 (7.2)	mg/mL

pK_a, acid dissociation constant.

concentrations of miltefosine was observed for both skin and plasma (coefficient of variation percentages of 65.9% and 39.5%, respectively). The median individual concentration ratio of skin to plasma was 1.19 (IQR: 0.79–1.9). In total, 17 patients had a ratio of skin to plasma <1, while 35 had a ratio >1. Individual plasma and skin miltefosine concentrations collected at the same time point exhibited a moderate degree of correlation with a correlation coefficient of 0.53. The median miltefosine skin concentrations in patients defined as responders at the 12-month follow-up visit was 48.7 µg/g (IQR: 20–71.9 µg/g), whereas for non-responders this was 42 µg/g (IQR: 28.8–58.5 µg/g), which was not significantly different (*P*=0.8).

Miltefosine PBPK model and simulations

A summary of the model parameters used in the drug model are given in Table 2. Simulated PK parameters are given in Table 3. Identified parameters are in line with previous reports and are summarized in Table 4. Skin concentrations were used to estimate parameters for the cell membrane binding partner (Table 4). The developed model adequately predicted typical miltefosine concentrations in the two compartments for which observations were available, i.e. plasma and skin. Accumulation of the drug in the skin exceeded concentrations in plasma, as illustrated in Figure 2, which is in line with higher median observations of miltefosine in the skin than in plasma. The model-based simulations indicated that the residence time of miltefosine in the skin is more than twice longer than the residence time in blood plasma, as estimated by a mean residence time (MRT) for the skin of 604 hours compared to 266 hours in plasma. The established PBPK model can be used to derive predicted exposure of other tissues of interest, which should be validated further (Figure 3). Simulated PK parameters for the spleen and liver are further summarized in Table 3. Last, the PK target for miltefosine in VL has been previously suggested as the time the miltefosine concentration is above the *in vitro* susceptibility EC₉₀ value of 10.6 mg/L.¹⁴ Present data indicate that 87% of PKDL patients had exposure in the skin above this target value. Typical time > EC₉₀ in the skin as simulated by the PBPK model was 52 days (from day 2 until day 54).

Discussion

In this study, we quantified miltefosine exposure in the skin following an allometric weight-based dosing regimen of 21 days

Table 3. Simulated pharmacokinetic parameters of miltefosine following the dosing regimen used in the clinical studies

Global PK analyses		
Parameter	Value	Unit
V_{ss} (plasma)	690	mL/kg
V_d (plasma)	788	mL/kg
V_{ss} (phys-chem)	633	mL/kg
Total plasma clearance	0.04	mL/min/kg
Plasma PK		
C_{max}	74	$\mu\text{mol/L}$
T_{max}	576	hours
AUC_{tEnd}	2.8×10^6	$\mu\text{mol} \times \text{min/L}$
Elimination half-life	210	hours
MRT	266	hours
V_{ss} (plasma)/F	691	mL/kg
Skin PK		
C_{max}	100	$\mu\text{mol/L}$
T_{max}	576	hours
AUC_{tEnd}	4.8×10^6	$\mu\text{mol} \times \text{min/L}$
Elimination half-life	211	hours
MRT	604	hours
Spleen PK		
C_{max}	93	$\mu\text{mol/L}$
T_{max}	576	hours
AUC_{tEnd}	3.6×10^6	$\mu\text{mol} \times \text{min/L}$
Elimination half-life	210	hours
MRT	265	hours
V_{ss} (plasma)/F	545	mL/kg
Liver PK		
C_{max}	133	$\mu\text{mol/L}$
T_{max}	576	hours
AUC_{tEnd}	5.1×10^6	$\mu\text{mol} \times \text{min/L}$
Elimination half-life	210	hours
MRT	265	hours
V_{ss} (plasma)/F	381	mL/kg

V_{ss} , volume at steady state; C_{max} , maximum (compartment) concentration; T_{max} , the time to reach C_{max} ; AUC_{tEnd} , area under the concentration-time curve until the end of treatment; MRT, mean residence time.

Table 4. Optimized model parameters of the full PBPK model based on the clinical observations of miltefosine in skin and plasma

Optimized parameter	Value	Unit
Physiochemistry		
Lipophilicity	3	log
Specific intestinal permeability	1.5	cm/min
CL_{spec}^a	3.17×10^{-3}	1/min
Cell membrane binding partner		
K_d	1 (fixed)	$\mu\text{mol/L}$
k_{off}	101.8	1/min
Reference concentration	56.95	$\mu\text{mol/L}$

K_d , equilibrium constant; k_{off} , dissociation constant.

^aSpecific clearance normalized to the enzyme concentration of 1 $\mu\text{mol/L}$.

in PKDL patients treated with a combination of LAmB and miltefosine therapy. Several dosing regimens have previously been evaluated for miltefosine in the treatment of VL, such as the conventional linear weight-based dosing (2.5 mg/kg/daily for 28 days) or an allometric weight-based dosing (up to 3.9 mg/kg/day for 28 days), whereas for PKDL a considerably longer 12 weeks of miltefosine treatment is recommended in Asia. This study provides the first evidence of miltefosine skin exposure and target site PK in PKDL, which, together with data about parasitological and clinical responses to treatment, will be of crucial value for future optimization and rationalization of miltefosine treatment in PKDL.

Miltefosine concentrations in the skin were highly variable between patients, which has also been observed for miltefosine in plasma in various studies.¹²⁻¹⁴ Empirical PK modelling could not be used to further characterize the skin PK of miltefosine, since skin concentration measurements were only available at a single time point. Therefore, we applied more advanced methods of PBPK modelling using drug- and system-specific information to further predict skin PK. Furthermore, this approach allowed us to characterize target site PK (e.g. MRT), parameters that could not otherwise be derived from a single observation.

In this study, 87% of patients achieved the PK target in the skin, in line with previous evaluations of the allometric weight-based dosing regimen in plasma,^{12,14} suggesting that this dosing regimen achieves sufficient target exposure of the parasites in skin tissue, also after 21 days. Since the target was defined based on the concentration of miltefosine required to induce intracellular susceptibility of *Leishmania donovani*, it could be assumed that such exposure would be sufficient to kill the same parasite localized within the dermis for PKDL patients. Extrapolation of these findings to other cutaneous forms of leishmaniasis such as CL remains difficult due to differences in susceptibility of the causative parasite species (e.g. an EC_{50} value of 11.82 mg/L for *L. major* in CL),³² as well as pathophysiological and morphological differences of the lesions potentially affecting target site accumulation.

Owing to the invasive nature of the biopsy sampling method and concerns about flare-up of the skin infection when sampled, sampling of the lesion area itself was not considered possible and led to a minimal sampling schedule of one sample per patient. Therefore, assessing drug exposure between infected and non-infected skin was not feasible in this clinical trial. This precluded feasibility of a longitudinal individual patient evaluation of target exposure attainment over time. Given the high correlation observed between the miltefosine plasma and skin concentrations, plasma concentrations could potentially serve as a surrogate marker for skin target concentrations. However, caution is warranted due to the large between-subject variability in the concentration ratio of skin to plasma.

We also developed a PBPK model for miltefosine, used to predict concentrations in the organs known to be affected by *Leishmania* parasites. Using the skin concentrations and pooled plasma concentration data, we were able to inform the PBPK model and introduce a cell membrane binding partner to represent the membrane binding capacity. It is expected that this cell membrane binding property is not tissue specific for miltefosine. The mechanism of miltefosine binding to membranes would be similar for all cell types, thus the extent of membrane

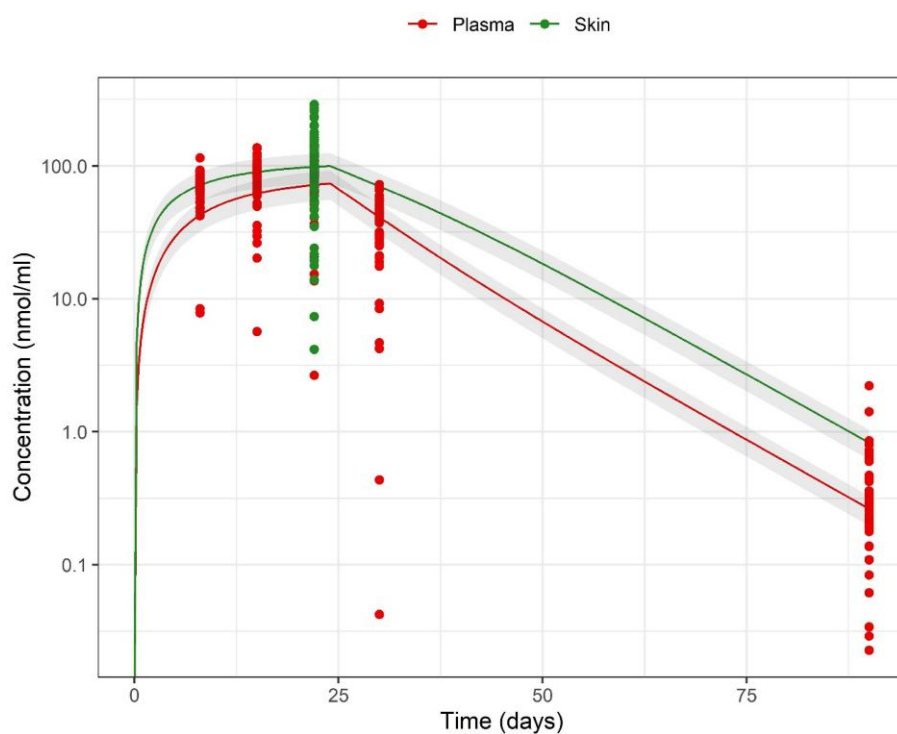


Figure 2. Observed and simulated miltefosine concentrations in plasma and skin tissue. Red dots represent observed concentrations in plasma and the red line represents a model simulation of miltefosine in plasma. Green dots represent observed miltefosine concentrations in the skin and the green line illustrates the simulated skin concentration based on the PBPK model. Shaded areas indicate 95% CI of the mean. This figure appears in colour in the online version of *JAC* and in black and white in the print version of *JAC*.

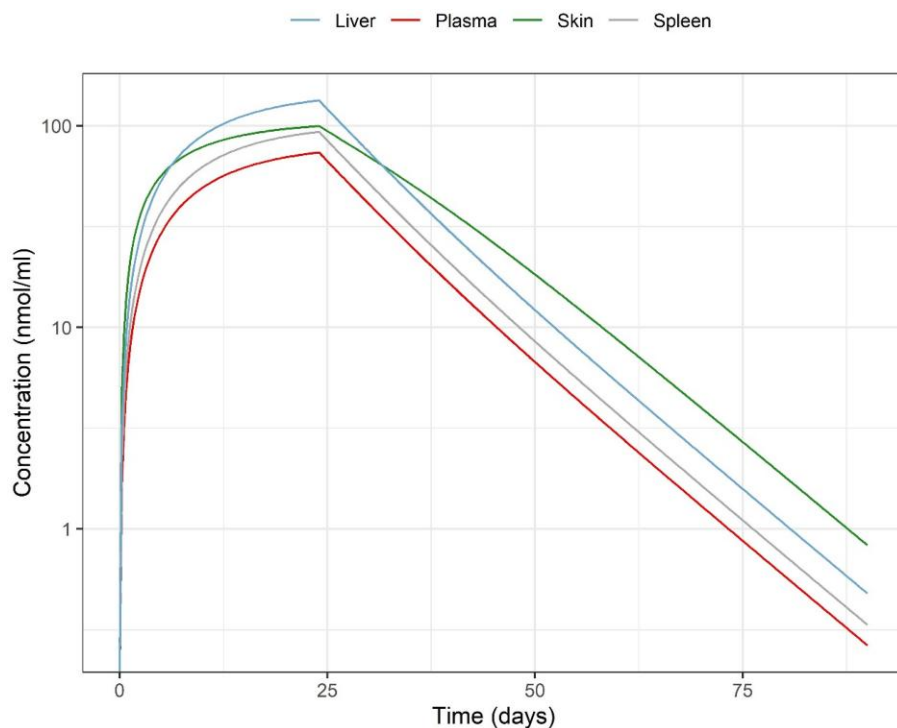


Figure 3. Model-based simulations of miltefosine pharmacokinetics in various organs following allometric weight-based dosing regimen in duration of 21 days. Blue line shows the liver; red line, plasma; green line, skin and the grey line, the spleen. This figure appears in colour in the online version of *JAC* and in black and white in the print version of *JAC*.

binding would be related to the number of cells in any compartment. Nonetheless, in having limited data to validate this model, further simulated exposures in spleen and liver should be interpreted with caution. The PBPK model-based predicted concentration–time curve in the skin suggests that typical target attainment ($T > EC_{90}$) after this 21-day regimen is twice as high (52 days) as the previously reported $T > EC_{90}$ values in plasma of VL patients treated for 28 days (24–27 days).^{12,14}

In conclusion, we demonstrated that miltefosine penetrates extensively into the skin after oral administration and that skin concentrations are potentially high enough to exert activity on the dermal parasites in PKDL. This study bridges the knowledge gap about miltefosine disposition in human skin and provides a promising start for future optimization of miltefosine in the treatment of PKDL. The PBPK model allows for the prediction of miltefosine concentrations in various other affected organ tissues such as the spleen and liver in VL, which are complicated to sample and collect in patients. This study highlights the feasibility, significance and importance of studying target site PK in skin tissue of PKDL patients in a clinical trial context, and we recommend its implementation in future clinical trials on dermal forms of leishmaniasis such as PKDL and CL. In future studies, the insights and extrapolations from the model developed in this study could prove valuable for characterizing miltefosine exposure and the associated parasite clearance response in specific organs or tissues.

Acknowledgements

We thank the patients involved in this study, their families and communities, without whom this work would not have been possible; and all co-investigators, clinical trial monitors, nurses, laboratory personnel and staff at the clinical trial sites KAMRC, RMRI and icddr.

Funding

DNDi received financial support for this work from the following donors: French Development Agency (AFD), France; World Health Organization—Special Programme for Research and Training in Tropical Diseases (WHO-TDR); Swiss Agency for Development and Cooperation (SDC), Switzerland; Dutch Ministry of Foreign Affairs (DGIS), the Netherlands; UK aid, UK; Médecins Sans Frontières International; Médecins Sans Frontières Switzerland; and other private foundations and individuals. The findings and conclusions contained herein are those of the authors and do not necessarily reflect positions or policies of the aforementioned funding bodies. T.D. acknowledges funding from the Dutch Research Council (Nederlandse Organisatie voor Wetenschappelijk Onderzoek, Veni grant no. 91617140) and the Swedish Research Council (grant no. 2022-01251).

Transparency declarations

None to declare.

References

1 Alvar J, Vélez ID, Bern C *et al.* Leishmaniasis worldwide and global estimates of its incidence. *PLoS ONE* 2012; **7**: e35671. <https://doi.org/10.1371/journal.pone.0035671>

2 Eiras DP, Kirkman LA, Murray HW. Cutaneous leishmaniasis: current treatment practices in the USA for returning travelers. *Curr Treat Options Infect Dis* 2015; **7**: 52–62. <https://doi.org/10.1007/s40506-015-0038-4>

3 Torres-Guerrero E, Quintanilla-Cedillo MR, Ruiz-Esmenjaud J *et al.* Leishmaniasis: a review. *F1000Res* 2017; **6**: 750. <https://doi.org/10.12688/f1000research.11120.1>

4 Zijlstra EE, Musa AM, Khalil EAG *et al.* Post-kala-azar dermal leishmaniasis. *Lancet Infect Dis* 2003; **3**: 87–98. [https://doi.org/10.1016/S1473-3099\(03\)00517-6](https://doi.org/10.1016/S1473-3099(03)00517-6)

5 Ismail A, Khalil EAG, Musa AM *et al.* The pathogenesis of post kala-azar dermal leishmaniasis from the field to the molecule: does ultraviolet light (UVB) radiation play a role? *Med Hypotheses* 2006; **66**: 993–9. <https://doi.org/10.1016/j.mehy.2005.03.035>

6 Singh OP, Tiwary P, Kushwaha AK *et al.* Xenodiagnosis to evaluate the infectiousness of humans to sandflies in an area endemic for visceral leishmaniasis in Bihar, India: a transmission-dynamics study. *Lancet Microbe* 2021; **2**: e23–31. [https://doi.org/10.1016/S2666-5247\(20\)30166-X](https://doi.org/10.1016/S2666-5247(20)30166-X)

7 Mondal D, Bern C, Ghosh D *et al.* Quantifying the infectiousness of post-kala-azar dermal leishmaniasis toward sand flies. *Clin Infect Dis* 2019; **69**: 251–8. <https://doi.org/10.1093/cid/ciy891>

8 Dorlo TPC, Balasegaram M, Beijnen JH *et al.* Miltefosine: a review of its pharmacology and therapeutic efficacy in the treatment of leishmaniasis. *J Antimicrob Chemother* 2012; **67**: 2576–97. <https://doi.org/10.1093/jac/dks275>

9 Bäumer W, Wlaz P, Jennings G *et al.* The putative lipid raft modulator miltefosine displays immunomodulatory action in T-cell dependent dermal inflammation models. *Eur J Pharmacol* 2010; **628**: 226–32. <https://doi.org/10.1016/j.ejphar.2009.11.018>

10 Mukherjee AK, Gupta G, Adhikari A *et al.* Miltefosine triggers a strong proinflammatory cytokine response during visceral leishmaniasis: role of TLR4 and TLR9. *Int Immunopharmacol* 2012; **12**: 565–72. <https://doi.org/10.1016/j.intimp.2012.02.002>

11 Ménez C, Buysse M, Farinotti R *et al.* Inward translocation of the phospholipid analogue miltefosine across Caco-2 cell membranes exhibits characteristics of a carrier-mediated process. *Lipids* 2007; **42**: 229–40. <https://doi.org/10.1007/s11745-007-3026-8>

12 Palić S, Kip AE, Beijnen JH *et al.* Characterizing the non-linear pharmacokinetics of miltefosine in paediatric visceral leishmaniasis patients from Eastern Africa. *J Antimicrob Chemother* 2020; **75**: 3260–8. <https://doi.org/10.1093/jac/dkaa314>

13 Dorlo TPC, Huitema ADR, Beijnen JH *et al.* Optimal dosing of miltefosine in children and adults with visceral leishmaniasis. *Antimicrob Agents Chemother* 2012; **56**: 3864–72. <https://doi.org/10.1128/AAC.00292-12>

14 Dorlo TPC, Kip AE, Younis BM *et al.* Visceral leishmaniasis relapse hazard is linked to reduced miltefosine exposure in patients from Eastern Africa: a population pharmacokinetic/pharmacodynamic study. *J Antimicrob Chemother* 2017; **72**: 3131–40. <https://doi.org/10.1093/jac/dkx283>

15 Ramesh V, Katara GK, Verma S *et al.* Miltefosine as an effective choice in the treatment of post-kala-azar dermal leishmaniasis. *Br J Dermatol* 2011; **165**: 411–4. <https://doi.org/10.1111/j.1365-2133.2011.10402.x>

16 Sundar S, Olliaro PL. Miltefosine in the treatment of leishmaniasis: clinical evidence for informed clinical risk management. *Ther Clin Risk Manag* 2007; **3**: 733–40.

17 Ramesh V, Dixit KK, Sharma N *et al.* Assessing the efficacy and safety of liposomal amphotericin B and miltefosine in combination for treatment of post kala-azar dermal leishmaniasis. *J Infect Dis* 2020; **221**: 608–17. <https://doi.org/10.1093/infdis/jiz486>

- 18** Pandey K, Pal B, Siddiqui NA et al. A randomized, open-label study to evaluate the efficacy and safety of liposomal amphotericin B (AmBisome) versus miltefosine in patients with post-kala-azar dermal leishmaniasis. *Indian J Dermatol Venereol Leprol* 2021; **87**: 34–41. https://doi.org/10.25259/IJDVL_410_19
- 19** Rabi Das VN, Siddiqui NA, Pal B et al. To evaluate efficacy and safety of amphotericin B in two different doses in the treatment of post kala-azar dermal leishmaniasis (PKDL). *PLoS ONE* 2017; **12**: e0174497. <https://doi.org/10.1371/journal.pone.0174497>
- 20** Moulik S, Chaudhuri SJ, Sardar B et al. Monitoring of parasite kinetics in Indian post-kala-azar dermal leishmaniasis. *Clin Infect Dis* 2018; **66**: 404–10. <https://doi.org/10.1093/cid/cix808>
- 21** den Boer M, Das AK, Akhter F et al. Safety and effectiveness of short-course AmBisome in the treatment of post-kala-azar dermal leishmaniasis: a prospective cohort study in Bangladesh. *Clin Infect Dis* 2018; **67**: 667–75. <https://doi.org/10.1093/cid/ciy172>
- 22** CTR India. New treatment regimens for treatment of post kala azar dermal leishmaniasis patients in India and Bangladesh region. New Delhi Database Publication (India). 2017. Identifier CTRI/2017/04/008421 <https://trialsearch.who.int/Trial2.aspx?TrialID=CTRI/2017/04/008421>.
- 23** Roseboom IC, Rosing H, Beijnen JH et al. Skin tissue sample collection, sample homogenization, and analyte extraction strategies for liquid chromatographic mass spectrometry quantification of pharmaceutical compounds. *J Pharm Biomed Anal* 2020; **191**: 113590. <https://doi.org/10.1016/j.jpba.2020.113590>
- 24** DNDi-MILT/COMB-01-PKDL. An open label, randomized, clinical trial of two regimens to assess the safety and efficacy for treatment of PKDL patients in the Indian subcontinent (Trial Protocol). <https://dndi.org/wp-content/uploads/2023/04/DNDi-MILT-COMB-01-PKDL-Clinical-Trial-Protocol.pdf>.
- 25** Dorlo TPC, Van Thiel PPAM, Huitema ADR et al. Pharmacokinetics of miltefosine in old world cutaneous leishmaniasis patients. *Antimicrob Agents Chemother* 2008; **52**: 2855–60. <https://doi.org/10.1128/AAC.00014-08>
- 26** Dorlo TPC, Hillebrand MJX, Rosing H et al. Development and validation of a quantitative assay for the measurement of miltefosine in human plasma by liquid chromatography-tandem mass spectrometry. *J Chromatogr B Anal Technol Biomed Life Sci* 2008; **865**: 55–62. <https://doi.org/10.1016/j.jchromb.2008.02.005>
- 27** Roseboom IC, Thijssen B, Rosing H et al. Development and validation of an HPLC-MS/MS method for the quantification of the anti-leishmanial drug miltefosine in human skin tissue. *J Pharm Biomed Anal* 2022; **207**: 114402. <https://doi.org/10.1016/j.jpba.2021.114402>
- 28** R Development Core Team. *R: A Language and Environment for Statistical Computing*. R Foundation for Statistical Computing, 2015.
- 29** Willmann S, Lippert J, Sevestre M et al. PK-Sim®: a physiologically based pharmacokinetic ‘whole-body’ model. *Drug Discov Today BIOSILICO* 2003; **1**: 121–4. [https://doi.org/10.1016/S1478-5382\(03\)02342-4](https://doi.org/10.1016/S1478-5382(03)02342-4)
- 30** Willmann S, Höhn K, Edgington A et al. Development of a physiology-based whole-body population model for assessing the influence of individual variability on the pharmacokinetics of drugs. *J Pharmacokinet Pharmacodyn* 2007; **34**: 401–31. <https://doi.org/10.1007/s10928-007-9053-5>
- 31** Mondal D, Hasnain MG, Hossain MS et al. Study on the safety and efficacy of miltefosine for the treatment of children and adolescents with post-kala-azar dermal leishmaniasis in Bangladesh, and an association of serum vitamin E and exposure to arsenic with post-kala-azar dermal leishmaniasis: an open clinical trial and case-control study protocol. *BMJ Open* 2016; **6**: e010050. <https://doi.org/10.1136/bmjopen-2015-010050>
- 32** Van Bocxlaer K, Caridha D, Black C et al. Novel benzoxaborole, nitroimidazole and aminopyrazoles with activity against experimental cutaneous leishmaniasis. *Int J Parasitol Drugs drug Resist* 2019; **11**: 129–38. <https://doi.org/10.1016/j.ijpddr.2019.02.002>